2001-01-3015

An Improved Procedure for Prediction of Drag Polars of a Joined Wing Concept Using Physics-Based Response Surface Methodology

Sriram K. Rallabhandi, Erol Cagatay ‡
Dimitri N. Mavris †

School of Aerospace Engineering
Georgia Institute of Technology
Atlanta, GA 30332-0150

ABSTRACT

Creation and utilization of accurate drag polars is essential in the aircraft sizing and synthesis process. Existing sizing and synthesis codes are based on historical data and cannot capture the aerodynamics of a non-conventional aircraft at the conceptual design phase. The fidelity of the aerodynamic analysis should be enhanced to increase the designer's confidence in the results. Hence, there is need for a physics-based approach to generate the drag polars of an aircraft lying outside the conventional realm. The deficiencies of the legacy codes should be removed and replaced with higher fidelity meta-model representations. This is facilitated with response surface methodology (RSM), which is a mathematical and statistical technique that is suited for the modeling and analysis of problems in which the responses, the drag coefficients in this case, are influenced by several variables. The geometric input variables are chosen so that they represent a multitude of configurations. Analytically created Response Surface Equations then replace the empirical aerodynamic relations and historical data found in sizing and synthesis codes, such as Flight Optimization System (FLOPS). The response surface equations obtained can be used in the system level studies and optimization. The approach described here is a statistics based methodology, which combines the use of Design of Experiments and Response Surface Method. Computational aerodynamic codes based on linearized potential flow (HASC) and boundary layer theory (BDAP) are employed to generate the needed parametric relationships. The aforementioned process is demonstrated through the implementation on a joined-wing concept.

INTRODUCTION

The main process flow in a typical preliminary design environment involves a complex inter-flow of information between various disciplines of the design. This traditional approach needs many iterations between the disciplinary analysis and system level analysis for arriving at the final design configuration.

The ability to perform quick design studies of many different configurations is very essential in a preliminary design environment because system level tradeoffs are needed in the initial phases of design. The paradigm shift in design has called for an increased knowledge of the problem at hand in the initial phases of design. Therefore a preliminary design environment is needed wherein the disciplinary analysis needs to be carried out in an accurate manner reflecting the physics of the problem, rather than using historical databases especially for radically different configurations. ASDL at the Georgia Institute of Technology has used vortex lattice analysis codes in conjunction with RSM for a few years now. As far as aerodynamics is concerned, accurate and rapid determination of drag polars for all the design configurations requires the use of reduced order models. These aerodynamic drag polars are then incorporated into the sizing and synthesis codes for system level tradeoffs.

The idea behind using reduced order meta-models is to cut short the computational time needed in the preliminary design phase. Various meta-models like the Response Surface Equations, Neural networks, etc. can be used. But for the purpose of the present study, Response Surface Equations have been used as the meta-model.

---

‡ M.Sc. Candidates, SAE Student Members
† Associate Professor, Director ASDL, Boeing Chair in Advanced Systems Analysis, SAE Member

The Response Surface Equations are produced by running aerodynamic analysis codes

according to the pattern laid down in the Design of Experiments (DOE) array, and subsequently incorporated in the sizing and synthesis codes. If all the disciplinary codes are run in this way and finally fused together in the sizing and synthesis codes, a concurrency in the final analysis is achieved and the iteration between the synthesis codes and the disciplinary codes is avoided. Use of RSEs and DoE also greatly enhances the speed and flexibility of the whole process. The RSE generation phase uses linearized aerodynamic codes.

METHODOLOGY

The design space of an aircraft is defined by a number of vehicle geometry variables, scaling parameters, and mission parameters. Each of these can be varied continuously over a wide range of values, and, quite often, multiple combinations of design space variables yield feasible and viable vehicles. The designer determines which vehicle is the best for a given set of requirements. This can be done using a multitude of optimization techniques, optimizing either to single or multiple attributes.

A wide array of analysis tools is available to evaluate aircraft size and performance at any specified setting of design variables. However, the design space is not simply a collection of points; it is rather a continuous space of vehicle attributes based on multiple variables. Therefore, the designer must create some sort of regression to take full advantage of the optimization techniques available. Furthermore, the designer may wish to view the vehicle attribute trends as a function of the design variables without running a cumbersome analysis code for every setting. Several multivariate regression techniques are available, but the most promising for aircraft systems seems to be Response Surface Methodology i.e. RSM **[1]**. This is a multivariate regression technique based on Design of Experiments (DoE) **[2]** methodology. A DoE is an ordered set of experiments designed to minimize the number of cases needed to provide a multivariate regression polynomial equation while ensuring that these variables are not correlated with each other.

Using RSM, the designer picks any number of responses and creates simple mathematical models for each response as a function of the design variables. Response Surface Methodology typically uses second-order quadratic equations of the form

$$R = b_0 + \sum_{i=1}^{k} b_i x_i + \sum_{i=1}^{k} b_{ii} x_i^2 + \sum_{i=1}^{k-1} \sum_{j=i+1}^{k} b_{ii} x_i x_j \quad (1)$$

where R is the response, b_0 is an intercept term, b_i are regression coefficients for the first-degree terms, b_{ii} are coefficients for the quadratic terms, b_{ij} are coefficients for the cross-product terms, and x_i is the i_{th} control variable.

This regression, known as a Response Surface Equation (RSE) is able to model linear effects through the linear terms, curvature effects through the quadratic terms, interaction effects through the cross-product terms, and effects not related to the control variables through the intercept term. This makes it a robust model for most sophisticated analysis codes that can run in a fraction of a second versus the several seconds to hours, which are typical of most analysis tools. RSM was employed throughout this study as a rapid space investigation and visualization technique.

COMPUTATIONAL ARCHITECTURE

Vortex lattice methods and boundary layer methods have been used in this study to predict the induced and the skin friction drag respectively. Vortex lattice method is based on solution to the Laplace equation, and is subject to the same basic theoretical restrictions that apply to the panel method. There are many different vortex lattice schemes, but in this section the classical interpretation has been described. Knowing that vortices can represent lift from the potential flow theory, the following procedure in a typical vortex lattice code was employed **[3]**:

1. Divide the wing planform into a lattice of quadrilateral panels, and place horseshoe vortices on each panel.
2. Place the bound vortex of the horseshoe vortex on the midpoint of the ¼ chord element line of each panel.
3. Place the control point on the ¾ chord point of each panel at the midpoint in the spanwise direction.
4. Determine the strength of each vortex required to satisfy the boundary conditions by solving a system of linear equations.

A full-blown CFD analysis is not appropriate for the preliminary design stage because quick and reasonably accurate data is needed.

COMPUTATIONAL AERODYNAMICS

An analytical procedure had to be developed in order to perform the aerodynamic analysis. Since the empirical method was dismissed as being too inaccurate for the requirements and also for not being suitable for any non-conventional design such as a joined-wing, a physics-based analysis method had to be chosen. Perhaps the most advanced aerodynamic tool used today is Computational Fluid Dynamics (CFD). CFD analysis gives accurate results and any design, including a joined-wing. The disadvantage of the CFD tool is that it is computationally very intensive. Using the RSE methodology with CFD modeling would take up quite a long time since hundreds of cases might have to be run. From a practical point, multiplying the computational time for one case with a few hundred would be overwhelming for the computer power available today. It was decided that potential flow would be the best analysis method for the considered approach. The accuracy of potential software tools would be acceptable for conceptual and

preliminary design. The assumptions for the potential flow method are as follows: Inviscid attached flow, Small angle-of-attack and planar panel method.

The two software packages used for the aerodynamic analysis were BDAP (Boeing Design and Analysis Program) and HASC (High Angle-of-Attack Stability and Control.)

BDAP

BDAP **[4]** was created by the Boeing Company and is used to calculate skin-friction drag. The code is a collection of several aerodynamic analysis programs based on linearized aerodynamics. The code is capable of analyzing the skin friction of three dimensional, multi-component bodies by using the turbulent flat plate theory method by near field drag calculation subroutine. Fully turbulent flow is assumed in this theory, so the skin-friction drag is over-estimated. However, the overestimation may compensate for the lack of consideration of the interference drags caused by protrusions on the actual aircraft such as the control surface deflection, doors or the windows. The important BDAP output was the skin-friction drag coefficient, which is generated while reflecting changes due to altitude and Mach number.

HASC

HASC **[5]** is a conceptual/preliminary design level aerodynamic prediction code. Semi-empirical methods are used to estimate the effects of vortex lift and breakdown. Output files provide information on the overall configuration, component loads, and vortex characteristics. The HASC code is primarily an integration of three routines:
VORLAX: A generalized vortex lattice program
VORLIF: A semi-empirical strake/wing vortex analysis code
VTXCLD: A two-dimensional, unsteady, separated flow analogy program for analyzing smooth forebody shapes
The tool is found to be very sensitive to the paneling on the surfaces, the suction parameter and the camber definition of the airfoil. The tool is found to produce good results at subsonic mach numbers. As the Mach number is increased to transonic values, the expected induced drag rise was not observed. HASC produces all the force and moment coefficients using which static and dynamic stability of the configurations can be studied.

CODE APPLICATION

This study was done as Aerodynamics part of the project in response to the AIAA/NAVY RFP **[6]** for the Common Support Aircraft (CSA). The United States Navy currently uses four aircraft in what are considered support roles. These are the E-2C Hawkeye for Airborne Early Warning (AEW), the S-3B Viking for Anti-Submarine Warfare (ASW), the ES-3A Shadow for Electronic Surveillance (ES), and the C-2A Greyhound for Carrier On-board Delivery (COD). These four aircraft originated from two basic airframes, so some spare parts and support equipment can be used interchangeably between the E-2C and C-2A, as well as between the S-3B and ES-3A. Each of these aircraft is nearing the end of its service life, so a new vehicle is required. This vehicle is the Common Support Aircraft (CSA), an aircraft envisioned to replace these four legacy aircraft with a single airframe and as few variants as possible. It should perform all four support missions to maximize affordability, defined as a measure of performance weighed against relative cost.

Thus, there is a great need to design an aircraft that utilizes the commonality between the different missions. An ultimate design would be one that has one airframe and one variant. In this scenario, the solution would be to eliminate the dome (AEW mission) entirely and integrate sensors into the airframe. This requires a configuration that lends itself to placement of sensors such that 360-degree coverage is possible. These sensors must be chosen such that synergy of mission-specific transmitting and receiving requirements is obtained. In this fashion, other internal mission equipment can be made modular so only one variant of the CSA is required. This is not a new idea, as the Boeing EX **[7]** and the NASA joined-wing demonstrator of **[8]** are both attempts to accomplish an AEW-like mission with all sensors integrated into the diamond-like joined wing planform, giving 360-degree coverage. This appears to be the best configuration for an all-around integrated sensor platform, so it is a concept worthy of further investigation.

The joined wing configuration, Figure **1**, is defined in **[9]** as an airplane that incorporates tandem wings arranged to form diamond shapes in both plan and front views. Advantages of the joined wing include: Light weight and high stiffness, low induced drag, good transonic area distribution, high trimmed C_{Lmax}, direct lift and side-force control capability, suitability for active aperture array radar in wings with 360-degree coverage.

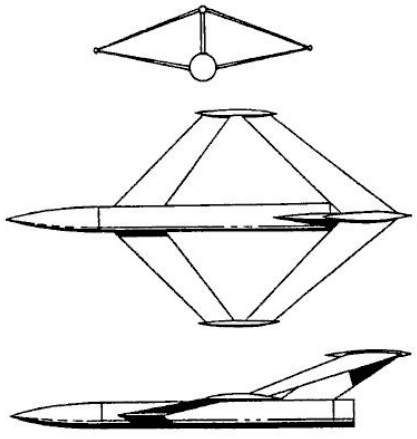

Figure 1. A typical joined wing configuration

CODE VALIDATION

Before the aforementioned aerodynamic codes were applied to the joined wing configuration, some

assumptions were necessary for the joined-wing aircraft. Some were due to geometric compatibility requirements. For example, rear wing root is located on the vertical tail. Therefore, the local vertical tail chord at this joint must equal the rear wing root chord. Other assumptions were simply limited by the data points given in the literature. For the joined wing, the following assumptions and relations were formulated:

- Gross Projected Area (GPA): S_R+S_F
- Quarter-chord sweep angle equality: $\Lambda_F = -\Lambda_R$
- Rear-to-front wing span ratio: $B = b_R/b_F$
- Rear-to-front wing area ratio: $S_{R/F} = S_R/S_F$
- Individual wing aspect ratio equality: $AR_F = AR_R$
- Corollary (area ratio relation): $S_{R/F} = B^2$
- Equivalent aspect ratio: $AR = b_F^2/GPA$
- Equality of thickness-to-chord ratio: $t/c_{avgF} = t/c_{avg\_R} = t/c_{avg\_VT}$
- Linearly-tapered wings
- Rear wing root chord equal to vertical tail chord at joint

Here, subscripts *F* and *R* denote front and rear wing, respectively. The joined wing configuration requires several new variables and compatibility relations. With these in mind, design space variables have to be chosen for parametric variation.

The induced drag coefficient decreases as the Mach number increases. As the Mach number of aircraft approaches Mach 1.0, the lift-curve slope increases as predicted by the Prandtl-Glauert rule. HASC uses leading edge suction in its analysis, which impacts the drag due to lift factor K. This quantity is given in **[10]** for subsonic Mach numbers as

$$K = SK_{100} + (1-S)K_0 \qquad (2)$$

where *S* is the percentage of leading edge suction, K_{100} is the *K* value for 100% suction, and K_0 is the *K* value for 0% suction. K_{100} is the inverse of the product of π and aspect ratio, and K_0 is the inverse of CL_α. Since CD_I is modeled as $CD_i = KCL^2$, increasing CL_α will increase K_0, which will consequently decrease CD_i. The output from HASC for the joined wing configuration at different Mach numbers is shown Figure **2**. This trend should reverse beyond the drag divergence Mach number, but this is not predicted by HASC. The data therefore needs correction above the drag divergence Mach number. The turbulent skin friction drag coefficient should decrease with increasing Reynolds number. Therefore, higher Mach numbers (and thus inertial forces) should reflect reduced skin friction drag coefficients. However, the zero-lift drag of the aircraft should increase at transonic Mach numbers (0.8 to 1.2) as shocks form on the wings and body. This additional drag due to compressibility, known as wave drag, was not accounted for by BDAP, so some correction had to be made to the output.

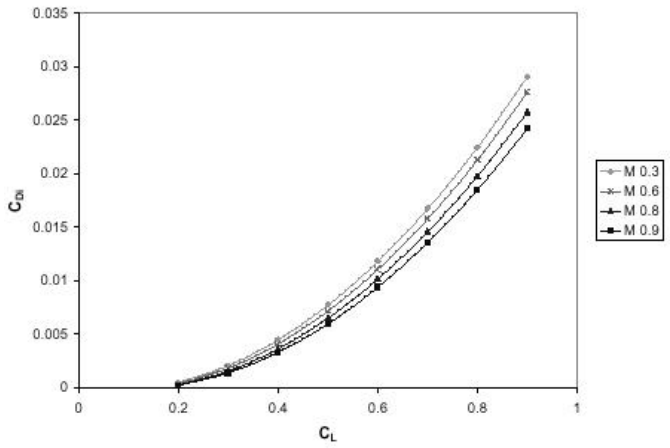

Figure 2. Induced drag from HASC for different M

The output from BDAP for the joined wing for two different altitudes is shown in Figure **3**.

Span ratio (B) has a large impact on the induced drag of a joined wing configuration **[11]**. A span ratio of 1 results in significant reductions to induced drag due to the endplate effect. Since the aspect ratios of both surfaces were constrained to be equal, the area ratio of the front and rear surfaces was simply the square of span ratio. Therefore, increasing the span ratio increases the area of the rear wing. A span ratio of one implies an area ratio of one, which can be considered a completely tandem wing system. In theory, a tandem wing has half of the induced drag of a single wing of equal gross projected area **[10]**. This result is not fully realized because the front wing contributes more to lift than the rear surface because, for trimmed flight rear wing operates in the downwash of the front wing. However, this general effect, combined with the endplate effect, contributes to

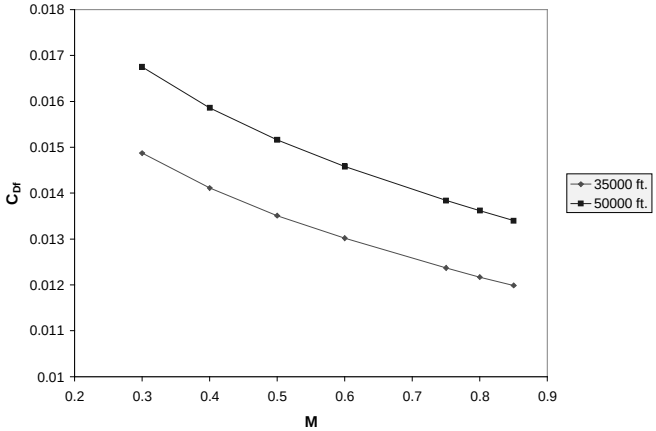

Figure 3. Effect of altitude on skin friction drag

significant savings in induced drag. The change in induced drag due to an increase in span ratio is depicted in Figure **4**. This chart shows that increasing span ratio reduces induced drag, as predicted.

Even though the results from the analysis tools do follow the expected trends, one cannot come to the conclusion that the computed results are correct. With little data

available on joined-wing aerodynamics, it's difficult to find ways to validate the output. However, observing the trends from these examinations are still steps taken in validating the data obtained, no matter how basic they may seem.

Though a lot has been talked about physics based modeling and prediction, some correction to the results, in the form of empirical corrections, was necessary for the transonic region. This is due to the unavailability of a

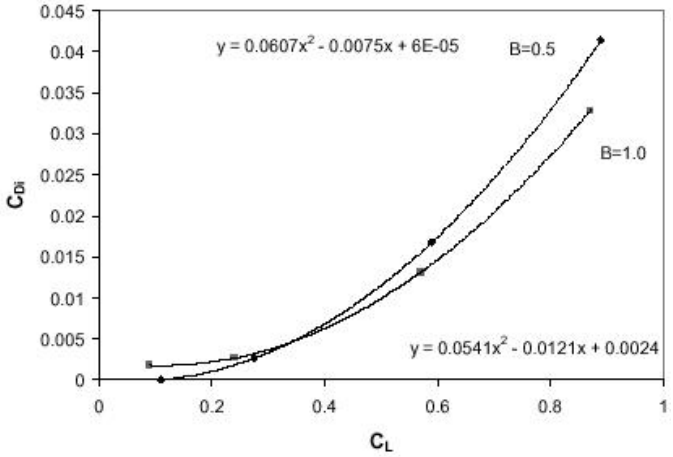

Figure 4. Effect of joint location on induced drag

transonic preliminary aerodynamic code. The critical Mach number was determined **[12]** and data points that lie on the transonic drag rise curve were calculated through a correlation to the Sears-Haack body wave drag and several assumptions regarding the geometry of the body **[10]**. By fitting a third-order polynomial through these critical data points, the additional drag was estimated at four Mach numbers. The increase in the drag coefficient of the final configuration due to compressibility effects is illustrated in Figure **5**. The critical Mach number *(M_{cr})* of the aircraft was calculated to be 0.77, and the drag divergence Mach number *(M_{DD})* 0.85. M_{DD} was chosen to be at a Mach number 0.08 higher than M_{cr} **[10].**

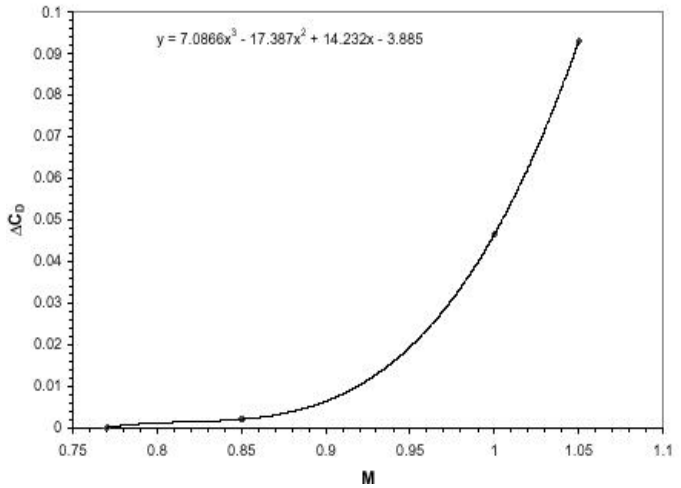

Figure 5. Transonic drag rise

The above codes have been used by many organizations and have been validated using experimental wind tunnel data. Hence no further validation was done on the codes.

SOLUTION PROCEDURE

Any analysis starts off with identifying the variables that can be perturbed and the responses that are desired. Since the final goal is to provide drag polars for the mission, all the necessary effects have to be identified as documented in Figure **6**.

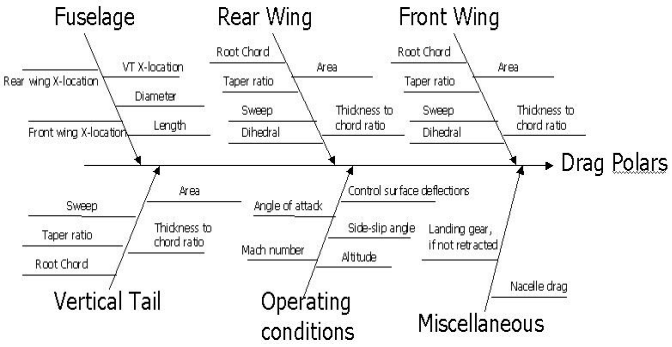

Figure 6. Cause and effect diagram

The ranges for the variables are selected in the conceptual design environment and used in the disciplinary analysis. Care is taken to see that the variable ranges are not too small or too large. Too small ranges render the RSEs inapplicable for larger design spaces, and large ranges make a poor fit. Final design variables and their ranges are provided in Table **1**.

Table 1. Variables and Ranges

Variable	Low	High	Units
Projected Area	500	700	ft^2
Dihedral Angle	0	10	Deg
Vertical tail sweep	-15	15	Deg
Vertical Tail area	35	70	ft^2
Vertical Tail Taper	0.3	0.7	
Wing Aspect Ratio	7	11	
Wing Taper	0.3	0.7	
Wing sweep angle	15	30	Deg
Wing t/c ratio	0.08	0.12	
Rear wing taper	0.3	0.7	
Tail joint fraction	0.5	1	
Front/rear span ratio	0.5	1	

The drag polar is expressed in the form,

$$C_D = C_{D_0} + K_0 + K_1 C_L + K_2 C_L^2 \qquad (3)$$

where C_{D0} the skin friction drag component, K_0 is the incremental profile drag due to lift, $K_1 C_L$ is an approximation of the interference drag and $K_2 C_L^2$ is the induced drag. C_{D0}, K_0, K1 and K_2 are functions of all key design parameters and flight conditions. RSEs were generated for K_1, K_2 and K_0 at each Mach number and for C_{D0} at each altitude. Thus 4 equations are generated for each flight condition. These equations are valid only for the chosen baseline configuration and the design

space around it as defined by the ranges selected for each of the independent variables.

COMPUTATIONAL MODELING

RSM was the essence behind the system of conceptual calculations for aerodynamics of the joined wing configuration. With the aid of a few aerodynamic software packages and RSM, the computed results could be easily placed into an input file for the FLOPS **[13]** design tool.

An analysis method was created to feed the necessary information into FLOPS. A separate DoE was created for the aerodynamic analysis that is a subset of the design space exploration DoE, since it only needed to include the variables that would have a visible effect on the aerodynamic performance of the aircraft in FLOPS. The variables obtained from the DoE are fed into the chosen aerodynamics codes for each configuration. A Java API, built for a conventional configuration and modified to handle the joined-wing configuration, was used to take information from the DoE and pass it to the input files for BDAP and HASC, changing the geometric settings for each case. In order to filter out data needed from the resulting output from the two aerodynamics codes, TCL/TK scripts for the UNIX operating system were used. The critical data values were then entered in JMP in order to generate RSEs JMP. This is shown diagrammatically in Figure **7**. The drag polar corresponding to the geometric variables in the design space exploration DoE is combined with the input file for that geometric configuration to create a final FLOPS input file. The aerodynamic DoE is a fractional factorial, resolution 5, 13 variable design array at three levels. This particular DoE has 153 different settings. Figure **8** illustrates the top view of some of the aerodynamics configurations considered with fuselage removed for clarity. Taper ratio, wing area, aspect ratio, span ratio, and sweep angle can be distinguished in this figure. This provides an excellent depiction of some of the outputs from the DoE table.

AIRFOIL SELECTION

The complex flowfield of the joined wing configuration makes standard methods for choosing an airfoil based on design lift coefficient impractical. The front wing causes downwash on the rear wing, and the rear wing induces upwash on the front wing. An airfoil from the NACA 642XX family has been shown **[9]** to be effective for joined wing aircraft at the preliminary design stage. CFD analysis can account for the curved flowfield around the wings. If this flowfield is quantified, a wiser choice can be made regarding the airfoil.

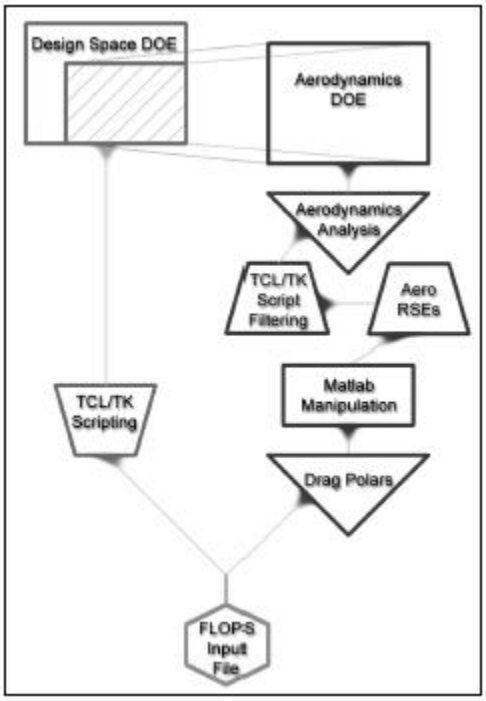

Figure 7. Aerodynamics analysis procedure

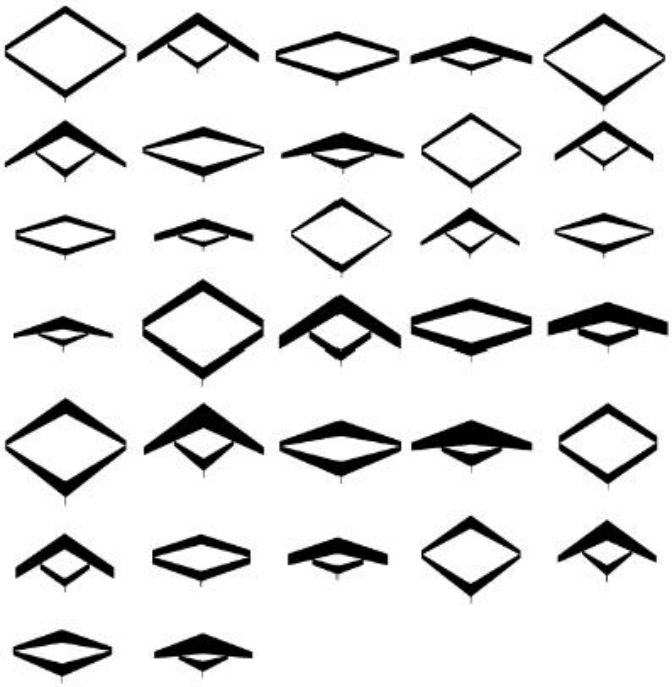

Figure 8. Sample planforms from the DOE

STABILITY ISSUES

The stability of the joined-wing configuration has to be handled in a different way as compared to conventional configuration. For a trimmed flight without any control surface deflection,

$$C_{m,CG} = C_{m,0} + \frac{dC_m}{dC_L} C_L = 0 \qquad (4)$$

here $C_{m,0}$ is the coefficient of pitching moment at zero lift condition. Since the pitch stiffness is required to be negative for static stability and C_L is positive for normal flight conditions, $C_{m,0}$ is required to be positive to satisfy the equation. The coefficient of pitching moment at zero lift can be defined as

$$C_{m,0} = C_{a,ac} + C_{m,stabilizer} + C_{m,\,fuselage} \quad (5)$$

For a joined wing, there is no horizontal stabilizer unlike the conventional configuration. Hence $C_{m,stabilizer}$=0. The fuselage contribution to C_m can be neglected which gives

$$C_{m,0} \cong C_{m,ac} > 0 \quad (6)$$

The twist provided to the joined wing helps achieve this condition. A rearward swept wing has tip-stall problems i.e. there is a span-wise flow out to the wingtips that pushes the lift distribution in that direction. Tip stall in rearward swept wings is caused due to the downwash from the wing, which causes the tip to see an effective higher angle of attack, which is the reason why the tip stalls first. Tip stall is bad because roll control is obtained from the ailerons mounted at wing tips. This is the reason that every rearward swept wing has "washout," i.e., the root incidence is greater than the tip incidence. However, this usually isn't so much of an issue with forward-swept wings, as these are typically canard configurations (or, in this case, the rear wing of a joined wing system). Forward swept wing stalls at the root before the tip. The root stall in case of forward swept wings can be explained by the downwash created at the root. So most forward-swept wings have "wash-in," i.e. the tip incidence is greater than the root incidence. Furthermore, **[9]** suggests that the incidence angle at the location where the wings get joined should be same for both the wings. Since the rear wing has less span when compared to the front wing, less twist is given so as to achieve an incidence of 0^0 for both surfaces at the joint location. Furthermore, wash-in can lead to structural divergence. Therefore, most forward-swept wings have just enough wash-in so the entire wing stalls at the same time or the root stalls just slightly before the tips.

As seen from Figure **9**, the washed out front wing and the washed in rear wing generate positive pitching moment around the CG.

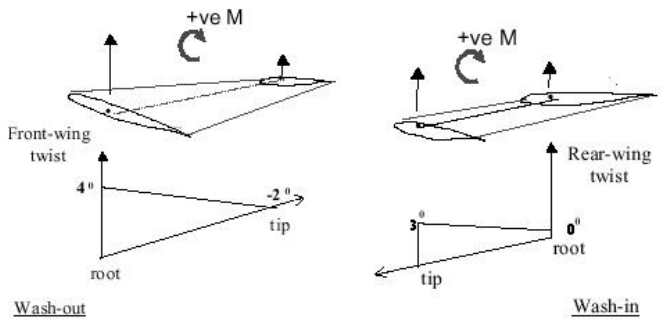

Figure 9. Twist distribution of joined wing

The above twist distribution provides necessary static stability for the aircraft as can be seen from Figure **10**. The picture on the left is for the untwisted configuration, which has a negative C_{m0} whereas for the twisted configuration, C_{m0} is found to be positive.

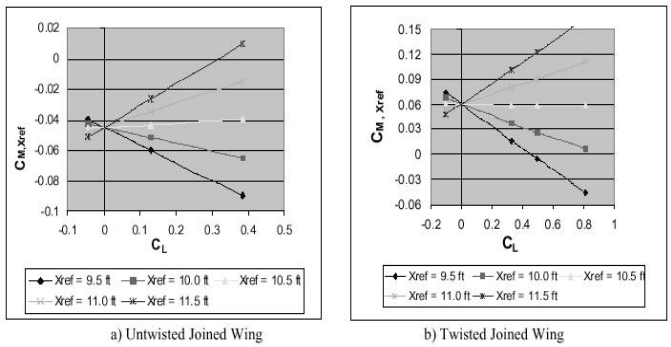

Figure 10. Effect of twist on moment coefficient

Also, the front wing has plenty of "aerodynamic wash-out" **[9]** in that the camber of the airfoil decreases towards the tip. The same is the case for the rear wing. This may be due to the effect of the interference between the two wings. The greatest changes in camber and incidence angle occur at the roots, where the fuselage or vertical tail meet with the wings, and toward the tips, where the wings join. This is most likely due to interference and tip vortex effects.

PLACEMENT OF CONTROL SURFACES

The placement of control surfaces is important because the paneling of the aircraft has to be changed for different positions of the control surfaces. The geometry of a joined wing aircraft enables placement of the control surfaces in various possible manners as discussed in **[11]**. The control surfaces are sized so as not to interfere with the wing box and to accommodate the integrated wing sensors. The locations of the aircraft's control surfaces on the wing can be observed in Figure 11. The flaperons (flap + aileron) on the front wing and the elevons (elevator + aileron) help achieve the direct sideforce capability to the aircraft. The drag rudders placed at the extreme outboard locations of the front wing provide additional yaw control to the aircraft and also serve as speed brakes during landing.

Wing Type	Control Surface Number	Type of Control Surface	Span-wise Length	Ratio to the main chord
Front	I	Slat	25.48%	0.10
	II	Flap	25.48%	0.20
	III	Flaperon	24.66%	0.20
	IV	Drag Rudder	10.73%	0.20
Rear	V	Elevator	25.48%	0.20
	VI	Elevon	24.66%	0.20

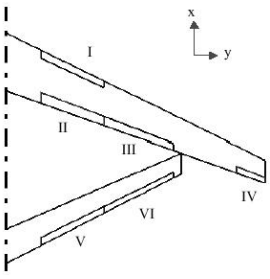

Figure 11. Control Surface Locations on Wing

HASC can predict the induced drag coefficients reasonably well even when the control surfaces are

deflected. The JAVA API was built in such a way that the paneling automatically changes whenever the size and deflection of the control surfaces are changed. The above placement of the control surfaces gives this configuration some unique characteristics like direct sideforce and direct lift **[9]**.

GENERATION AND VALIDATION OF RSEs

With the above background on the control surfaces, one could create RSEs with parametric control surface sizes and deflections. Though theoretically possible, the number of variables increases beyond the number that the present tools can handle. For this reason RSEs were generated using a clean configuration, i.e. with assumed control surface sizes and zero deflections. The Response Surface Equations were generated using the statistical software package JMP **[14]**. To assess the accuracy of these equations with respect to the codes that created them verification tests have to be performed. The R^2 fit measures the variation of the fit with respect to the measured points. Random cases may be run and the responses from the analysis may be compared to the values predicted by the RSEs. And finally, a residual plot, which shows the error distribution of the RSE regression, should not show a pattern and should be random. In the present case, all the three tests were satisfactory and the RSEs were a true representation of the actual analysis codes being used.

The R^2 values obtained for each of the RSEs exceeded 0.99 for all cases. Residual plots should show a random scatter. A residual plot, Figure 12, was used to observe the error distribution of the RSE regression for K_2 at M=0.6. Good R^2 values and a random residual plot do not guarantee good fits of RSEs for points falling anywhere between the lower and higher limits. For this reason 153 random cases were considered within variables ranges. The responses are calculated from the aerodynamic codes as well as the RSEs. The predicted values of K_2 at M=0.6 against values from the analysis codes are presented in Figure 13. The solid line is the ideal fit and deviations from this line are a measure of the confidence interval of the RSEs.

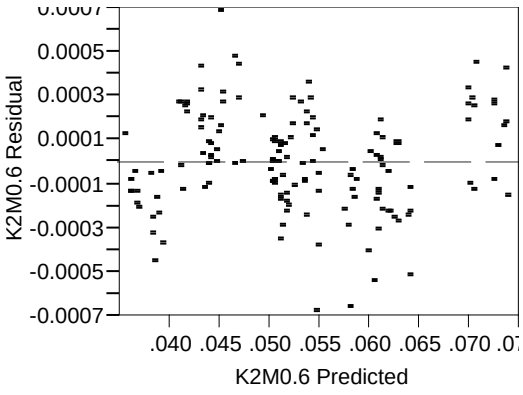

Figure 12. Error distribution of K_2 regression

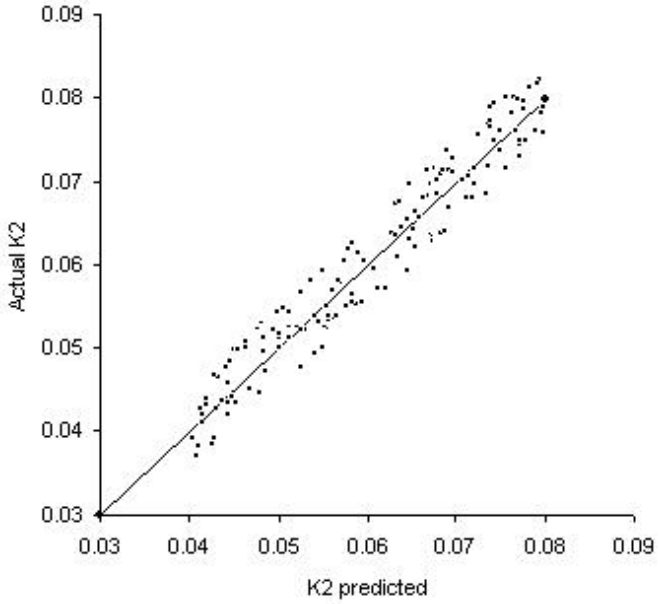

Figure 13. Difference between predicted and actual K_2 values

Almost all the points lie within a small corridor and the RSEs can be used to predict the drag values obtained from the analysis codes.

FINAL OPTIMIZED CONFIGURATION

A MATLAB program was written for the design space to optimize the configuration for minimum life cycle cost with a set of constraints. The final optimized configuration is illustrated in Figure 14.

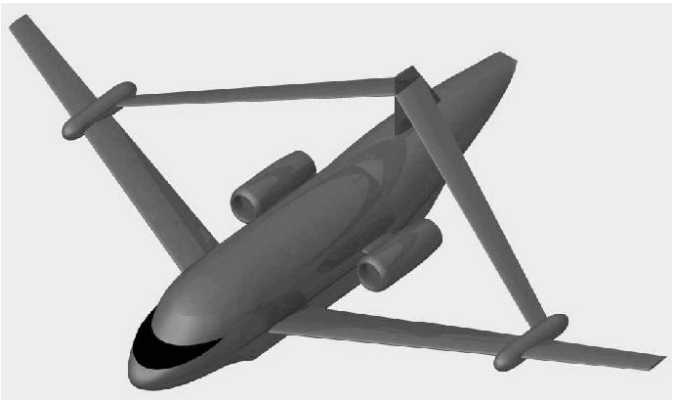

Figure 14. Final optimized joined wing aircraft configuration

The final optimized configuration was analyzed by employing the mentioned methodology. As a result, the drag coefficients for the aircraft were obtained. The drag polars for the final optimized configuration can be seen in Figure 15.

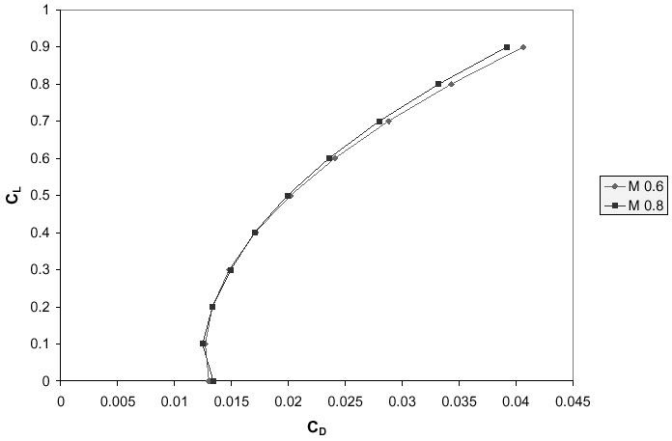

Figure 15. Drag polar of final optimized joined wing configuration

One important note about the final drag polars is that these are the results before the drag divergence sets in. Improved transonic drag prediction codes are required to predict the increase in drag above the drag divergence Mach number, which is beyond the scope of this work.

FUTURE WORK

RSEs work only under the hypothesis that the underlying aerodynamic behavior can be captured by a quadratic polynomial representation. RSEs fail to hold if this is not the case, in which case the error involved may be huge and higher order meta-models may have to be used. Either independent or dependent variable transformations can be used to achieve better results. Limitations of RSEs have to be overcome and better physics based methods like the neural networks have to be used to improve the whole process.

The aerodynamic analysis codes like HASC and BDAP, being linearized codes, have their own errors. Hence some other reduced order fast analysis codes can be designed. Preliminary wing optimization needs to be done and WINGDES as it is right now cannot handle vertical displacement of wings. Hence WINGDES has to be modified to handle a general wing configuration. A generalized tool for wing design and optimization, which can parametrically optimize a generalized wing, is needed to obtain the optimum twist distribution. High fidelity and fast transonic aerodynamic tools need to be used replacing subsonic analysis codes like HASC. A parametric CFD analysis with a multi-processor architecture would greatly benefit the aerodynamic design studies in the initial stages of a systems design environment.

CONCLUSIONS

The intention of this study was to generate a first order estimate of the drag characteristics of a non-conventional aircraft configuration such as the joined wing. Aerodynamic analysis modules within sizing and synthesis codes such as FLOPS have been enhanced by introducing RSEs in place of empirical relationships for drag calculation. RSEs are particularly suited for parametric studies because of their speed and flexibility. Linearized theory and boundary layer equations have been used in the computational environment. A reasonable disciplinary knowledge can be obtained in the preliminary design phase by following this method. Although RSEs have been generated only for aerodynamics here, the procedure is applicable to other disciplines as well. Fundamental disciplinary knowledge is thus obtained at a very early stage of the design, which paves way for a better final design with less cost.

ACKNOWLEDGMENTS

The authors wish to acknowledge the invaluable suggestions of Mr. Rob McDonald and Dr. Michelle Kirby. Special thanks are also due to Dr. Dan DeLaurentis, Mr. Nick Borer, Mr. Aditya Utturwar and other ASDL members for their help and support.

REFERENCES

1. Kirby, M. R., *A Methodology for Technology Identification, Evaluation, and Selection in Conceptual and Preliminary Aircraft Desig*n, Ph.D. Thesis, Georgia Institute of Technology, Atlanta, March 2001.
2. Box, G.E.P., Hunter, W.G., Hunter, J.S., Statistics for Experiments, John Wiley & Sons, Inc., New York, 1987
3. Miranda, L.R., Elliot, R.D., and Baker, W.M., "A Generalized Vortex Lattice Method for Subsonic and Supersonic Flow Applications", NASA CR-2865, 1977
4. Middleton, W. D., Lundry, J. L., Coleman R. G., "A Computational System for Aerodynamic Design and Analysis of Supersonic Aircraft, Part 2: User's Manual," NASA, 1976
5. Albright, A. E., Dixon, C. J., Hegedus, M. C., "Modification and Validation of Conceptual Design Aerodynamics Prediction Method HASC95 With VTXCHN," NASA, Virginia, March 1996
6. AIAA Foundation Graduate Team Aircraft Design Competition NAVY RFP, AIAA, 2000.
7. "Diamond Eyes", http://popularmechanics.com
8. "Joined Wing Integrated Structures Flight Demo", <www.dfrc.nasa.gov/Projects/revcon/joined.html>
9. Wolkovitch, J., "The Joined Wing: An Overview," AIAA Paper 85-0274, Jan. 1985
10. Raymer, D. P., *Aircraft Design: A Conceptual Approac*h, 3 rd ed., AIAA, Virginia 1995
11. Wolkovitch, J., "Joined-Wing Research Airplane Feasibility Study," AIAA Paper 84-2471, 1984
12. Torenbeek, E., *Synthesis of Subsonic Airplane Design,* Delft University Press, Delft, Holland 1982
13. McCullers, L. A., "Flight Optimization System, User's Guide," Release 5.94, Virginia, Dec. 1998
14. "JMP Version 4 User's Guide," SAS Institute, 2001

CONTACT

Any correspondence about this paper is welcome and can be addressed to:

Sriram Rallabhandi / Erol Cagatay, Aerospace Systems Design Lab, School of Aerospace Engineering, Georgia Institute of Technology, Atlanta, GA 30332-0150.

E-mail: sriramr@asdl.gatech.edu,erolc@asdl.gatech.edu